Proceedings of Global Power and Propulsion Society
ISSN-Nr: 2504-4400
GPPS Chania22
September 12 - 14, 2022
www.gpps.global

GPPS-TC-2022-0140

Numerical simulation of the solidification of a single molten droplet impinging on flat plate using multi-resolution MPS method

Shuma Kato
Graduate School of Mechanical Engineering
Tokyo University of Science
4522510@ed.tus.ac.jp
6-3-1, Niijuku Katsushika-ku, Tokyo, Japan

Koji Fukudome
Department of Mechanical Engineering
Tokyo University of Science
kfukudome@rs.tus.ac.jp
6-3-1, Niijuku Katsushika-ku, Tokyo, Japan

Makoto Yamamoto
Department of Mechanical Engineering
Tokyo University of Science
yamamoto@rs.tus.ac.jp
6-3-1, Niijuku Katsushika-ku, Tokyo, Japan

ABSTRACT

Particle deposition in a jet engine is a complex physical phenomenon that includes free-surface flow and phase changes. The moving particle simulation (MPS) method is extremely useful for numerical simulations, although it incurs high computational costs. In this study, we used the multiresolution MPS (MRMPS) method to simulate the deposition phenomenon of a liquid droplet to reduce the computational cost. When using the MRMPS method, we modified some conditions concerning the division of the computational particle. As a result, the spreading behavior and rim shape of a droplet impinging on a cold wall with solidification showed reasonable agreement with the experiment. In addition, this model has the advantage of reducing the computational time.

INTRODUCTION

When a jet engine inhales volcanic ash and sand while flying, the particles melt as they pass through a high-temperature combustion chamber. They then collide with the relatively low-temperature turbine blades, solidify, and deposit on the wall surface. This is known as the deposition phenomenon, which deteriorates the aerodynamic and film-cooling performance of jet engines. Therefore, predicting deposition phenomena is a critical problem in the design of jet engines. An experimental study of deposition requires handling high-temperature and high-pressure flow fields, and damaging the engine using particle ingestons is costly. Therefore, predicting deposition using numerical simulations is beneficial.

Many researchers have investigated the solidification process of molten droplets. Shakeri and Chandra (2002) observed the impingement and solidification of tin droplets on flat plates experimentally. They revealed the effect of the tin droplet's impinging velocity and surface roughness of the flat plates on the spreading and solidification processes. Ghafouri-Azar et al. (2002) investigated the interactions of multiple molten droplets impinging on a solid surface experimentally. Additionally, they performed numerical simulations using the volume of fluid (VOF) method. They revealed the effect of the distance between the impinging droplets and droplet solidification speed. Pasandideh-Fard et al. (2002) investigated the deposition of tin droplets on a stainless-steel surface experimentally and numerically. They developed a three-dimensional model of free-surface fluid flow accompanied by heat transfer and solidification and applied it to simulate the impact of a droplet on a flat substrate using the model of Bussmann et al. (Bussmann, 1999). Sundaram et al. (Sundaram et al., 2007) investigated the effect of deposition near the cooling hole and spallation of a thermal barrier coating. They revealed the relationship between deposition and endwall film cooling effectiveness.

In addition, numerical simulations of the deposition phenomenon were performed using the moving particle simulation (MPS) method. In the MPS method (Koshizuka and Oka, 1996, Koshizuka et al., 2018), the objective fluid is discretized by small computational particles, and each particle moves with its own velocity. Therefore, the MPS method is suitable for simulations of free-surface fluid flow. However, because of the large number of computational particles required to create

the entire flow field, it incurs a high computational cost. Therefore, some simulations were performed using the explicit moving particle simulation (E-MPS) method (Oochi et al., 2010), which is a type of MPS method that solves the pressure field explicitly using the number density distribution. Kondo et al. (Kondo et al., 2018) investigated three-dimensional numerical simulations of the deposition behavior of a single molten droplet on isothermal walls using the E-MPS method. They reproduced impingement and solidification processes. Fukudome et al. (Fukudome et al., 2021) investigated three-dimensional numerical simulations of the solidification behavior of molten droplets impinging on a non-isothermal wall using the E-MPS method. Their results showed reasonable agreement with the experimental data (Shakeri and Chandra, 2002).

Numerical simulations using the E-MPS method have several advantages, such as the application of a large deformation of the interface without constructing the grid system. However, the E-MPS method has a disadvantage in that the computational cost for increasing accuracy is higher than that of grid-based methods. To simulate the deposition phenomenon of jet engines, it is necessary to increase the numerical resolution owing to high-speed collisions, which results in a high computational cost. Therefore, it is helpful to reduce the computational cost by controlling the resolution by changing the diameter of the computational particles as necessary. In this study, a numerical simulation using the multi-resolution moving particle simulation (MRMPS) method (Tanaka et al., 2009) was performed for the deposition phenomenon, and the evaluation of the model on the division of a particle and the computational cost reduction was examined. The results of the present study show that MRMPS can significantly contribute to the reduction of computational cost and reproduction of small structures such as fingers.

METHODOLOGY

Multi-resolution MPS Method

We introduced the MRMPS method into E-MPS method. This method comprises of computational particles whose motion is based on the incompressible Navier-Stokes equations, equation of continuity, and equation of energy. The differential operators in the governing equations were discretized using particle interaction models (Koshizuka et al., 2018) such as gradient and Laplacian models.

In the MRMPS method, the resolution is varied by splitting and merging particles. In this study, only splitting was introduced to partially increase numerical resolution. Figure 1 shows the schematics in which one particle is split into two particles. The high- and low-resolution regions were set in advance, and splitting determination was performed on low-resolution computational particles that invaded the high-resolution region. The particle size after splitting was determined based on the number of splittings according to the mass conservation law. In this study, when splitting particle *i*, we consider the splitting direction vector for placing the particles after splitting, which is known as $\boldsymbol{t}_i^{\mathrm{SP}}$. To maintain the value of the particle number density close to that of the standard particle number density (i.e., satisfy the mass conservation law), it is desirable to determine the direction in which the gap is relatively large in the distribution of the surrounding particles. Therefore, it is necessary to evaluate the surrounding voids. The evaluation function used for the evaluation is expressed as e_i^{SP}. It is defined as follows:

$$e_i^{\mathrm{SP}} = \frac{1}{n_i} \sum_{j \neq i} \left| \frac{\boldsymbol{r}_{ij}}{|\boldsymbol{r}_{ij}|} \boldsymbol{t}_i^{\mathrm{SP}} \right| \tilde{w}_{ij}. \tag{1}$$

The diameter after splitting is expressed as follows:

$$d'_i = \frac{d_i}{2^{1/D_s}}. \tag{2}$$

The position and velocity of two splitted particles are expressed as follows:

$$\boldsymbol{r}'_i = \boldsymbol{r}_i \pm \frac{1}{2} d'_i \boldsymbol{t}_i^{\mathrm{SP}} \;\; ; \; \boldsymbol{u}'_i = \boldsymbol{u}_i. \tag{3}$$

In addition, when an appropriate $\boldsymbol{t}_i^{\mathrm{SP}}$ could not be uniquely determined, the splitting determination was made not to split particle *i*. We used e_i^{SP} as the criterion for the splitting determination (Tanaka et al., 2009), which is to search for an appropriate $\boldsymbol{t}_i^{\mathrm{SP}}$. The boundary values of e_i^{SP} used in the splitting determination are described in the next section.

In this study, we simulated a state in which a droplet solidifies while generating a liquid film after colliding with a cold flat plate. The computational particles change their phase based on the temperature, where the liquid and solid particles are above and below the melting point, respectively. We also dealt with intermediate phase particles, that is, transient phase particles, responsible for releasing latent heat at the melting point.

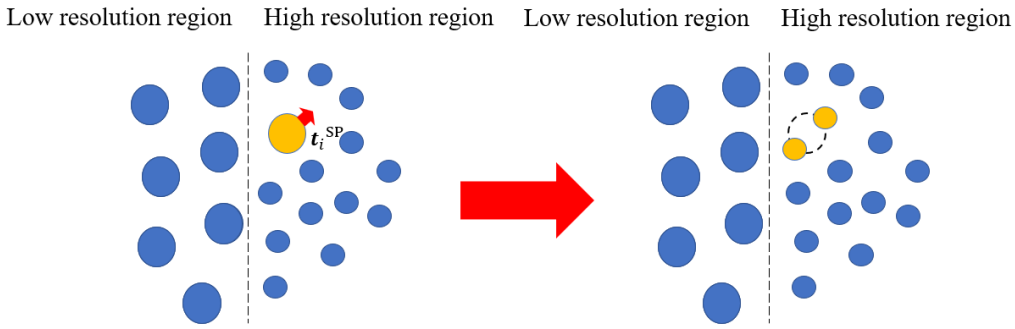

Figure 1 Schematics of splitting particle and splitting direction t_i^{SP}.

CALCULATION CONDITION

Figure 2 shows the schematic of the object used in this study. The initial conditions were as described by Shakeri and Chandra (2002). The initial droplet was completely spherical, with a diameter of 2.2 mm. A single tin droplet was placed 5 mm above the wall surface and dropped vertically. The initial velocity V_0 and temperature T_0 were 4.0 m/s and 519 K, respectively. The flat plate was made of stainless-steel with an initial temperature, T'_0 of 298 K.

We performed deposition simulations for Cases A, B, and C as listed in Table 1. In Case A, the initial diameter of a computational particle was 25.0 μm, and splitting was not considered. In Case B, the initial diameter was 25.0 μm, and splitting was considered. In Case C, the initial diameter was 20.0 μm, and splitting was not considered.

We set the splitting condition as a single computational particle split into two particles, and the particle diameter after splitting changed based on the mass conversation law. The splitting direction t_i^{SP} was determined in the case of $0.8 < e_i^{SP} < 1.3$. In the present study, we set the high-resolution region to reproduce the thinner liquid film apart from the center. When a computational particle exceeded a distance of 3.3 mm in the horizontal direction from the center of the initial droplet, splitting determination was carried out for the particle. In addition, based on n_{min} which is the minimum value of the particle number density in the initial particle arrangement, the splitting determination was carried out when the particle number density n_i of the particles that invaded the high-resolution region was $n_i < 2.43n_{min}$.

The melting point of tin T_{melt} is 505 K. All the other physical properties of the liquid and solid phase tins and stainless-steel plate (substrate) are shown in Table2. In addition, for the transient phase (i.e., solid-liquid phase particles), these physical properties were obtained by interpolating the solid and liquid phase values using the liquid fraction γ_m.

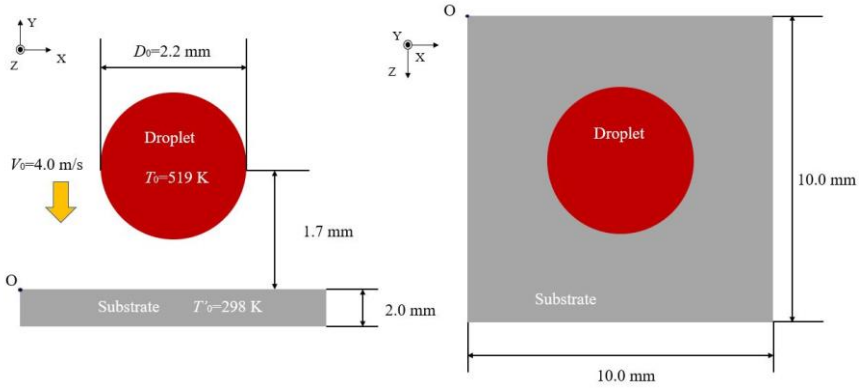

Figure 2 Schematic of the computational object displayed with the side (left) and top (right) views.

Table 1 Initial number of particles and the adaption of the splitting model.

Case	Computational particle diameter d_0 [μm]	Initial particle number	Splitting
Case A	25.0	388500	w/o
Case B	25.0	388500	w/
Case C	20.0	756000	w/o

Table 2 Thermal properties of tin for liquid, solid states, and stainless-steel substrate.

	k [W/(m·K)]	C [J/(kg·K)]	ρ [kg/m^3]
Liquid Tin	33.6	244	6980
Solid Tin	62.2	226	7200
Stainless Steel Substrate	14.9	477	7900

RESULTS AND DISCUSSION

Figure 3 shows the temporal behavior from droplet impingement to solidification for Cases A and B. In the figure red, white, and blue particles represent the liquid, transient, and solid phases, respectively. There is no significant difference between (a) and (b) in Figure 3 because splitting determination was not performed. In Figure 3 (c), some periphery solidification in Case B (right) is faster than that in Case A (left). Moreover, in Figure 3 (d), the finger shapes marked by the red arrows are similar to the experimental results (Shakeri and Chandra, 2002) at the periphery in Case B (right) compared with Case A (left).

We compared the spread factor in Figure 4 with the experimental data (Shakeri and Chandra, 2002). All of the present converged values after 2.5 ms show reasonable agreement with the experimental data, including the splitting case (Case B). Thus, it was confirmed that the evaluation of the final spread factor could be reproduced well even if the splitting calculation was introduced.

Table 3 shows CPU time for each case and eventual total number of particles. The CPU time of Case B is equivalent to approximately 230% of Case A. This is because the time is spent primarily on the process of splitting determination. Subsequently, the CPU time of Case B is equivalent to approximately 71.5% of Case C. In Case B, because the diameter of the particle after splitting changes to approxmately d_1= 19.8 μm, partial resolutions are considered to be comparable to those of Case C. Partially increasing resolution by introducing MRMPS method leads to reduce the computational cost rather than entirely increasing resolution. Therefore, it is confirmed that the splitting of the computational particles effectively reduces the computational cost.

On the contrary, by introducing splitting, we confirmed that nonphysical division can occur in case of not appropriate boundary value. Particles can be scattered discretely; conversely, the reproduction of the phenomenon can be inhibited. Then, it can especially take high computational cost to conduct the splitting determination. Therefore, we have to set the boundary value carefully.

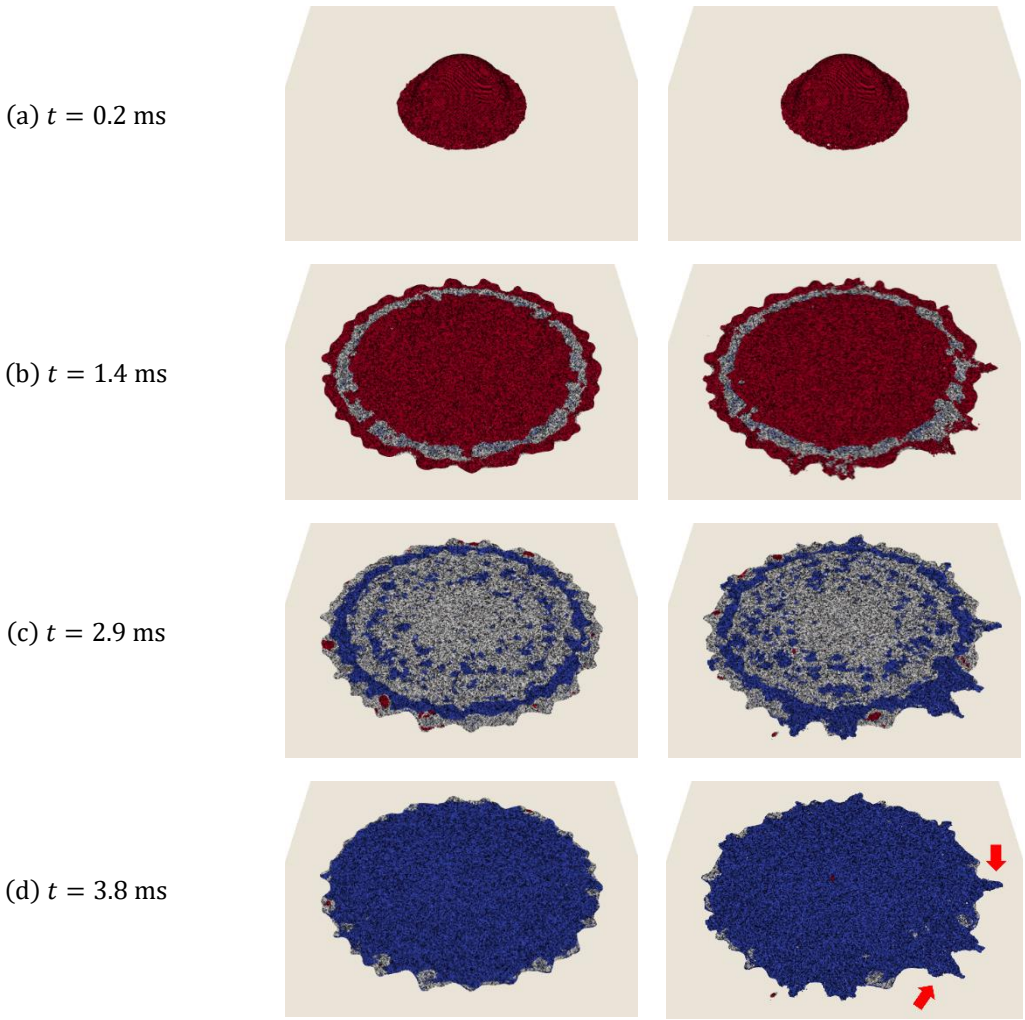

Figure 3 Solidification behaviour the impinging droplet. The left and right figures denote Case A and Case B from (a) *t* = 0.0 ms to (d) *t* = 0.9 ms.

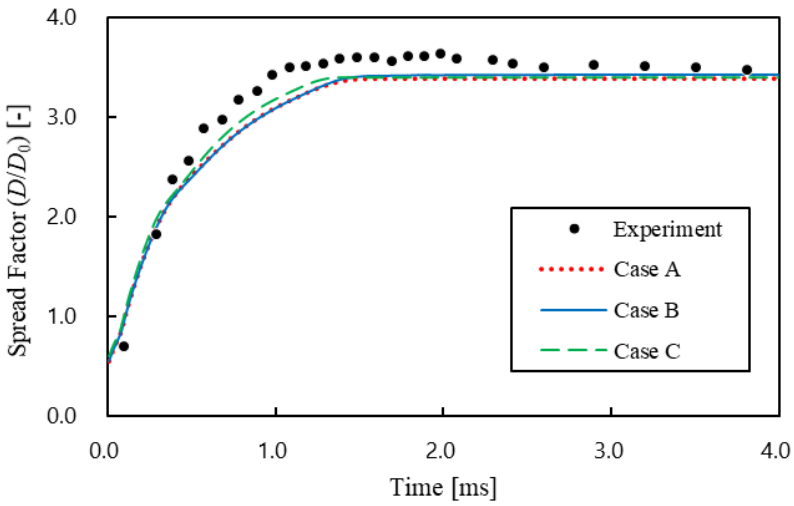

Figure 4 Time evolution of Spread Factor.

Table 3 CPU Time of simulation and number of increased particles.

	Case A	Case B	Case C
CPU Time [hrs.]	112	258	361
Number of Increased Particles	-	3,034	-

CONCLUSIONS

A numerical simulation of the deposition phenomena using the E-MPS method with the MRMPS method was performed to improve the simulation accuracy and reduce the computational cost. Consequently, the following insights were obtained:

1. The total computational cost was reduced using the MRMPS method. The spreading and solidification behavior was validated by comparison with experimental results.
2. By introducing splitting, the finger shape of the rim was well reproduced.
3. It was advantageous to select the particles to perform the splitting determination using the particle number density to reduce the calculation cost.

NOMENCLATURE

e^{SP}	Evaluation function [-]
$\boldsymbol{t}^{\mathrm{SP}}$	Vector for the arrangement of splitting particles [m]
n	Particle number of density [-]
$\boldsymbol{r}$	Position vector of the particle [m]
$\tilde{w}$	Weighting function for Multi-resolution MPS method[-]
d	Diameter of the particle [m]
$\boldsymbol{u}$	Velocity vector [m/s]
Ds	Dimension [-]
$()_{ij}$	Particle index
$()'$	Split particle index

ACKNOWLEDGMENTS

This work was partially supported by the Japan Society for the Promotion of Science (JSPS) KAKENHI Grant No. 20H04200.

REFERENCES

Bussmann et al. (1999). On a three-dimensional volume tracking model of droplet impact. *Physics of Fluids*, 11.6, pp. 1406–1417.

Fukudome, K. et al. (2021). Numerical simulation of the solidification phenomena of single molten droplets impinging on non-isothermal flat plate using explicit moving particle simulation method. *International Journal of Heat and Mass Transfer*, 180, 121810.

Ghafouri-Azar et al. (2002). Interactions between molten metal droplets impinging on a solid surface. *International Journal of Heat and Mass Transfer*, 46.8, pp. 1395–1407.

Kondo et al. (2018). Numerical simulation of solidification phenomena of single molten droplet on flat plate using E-MPS method. *Journal of Fluid Science and Technology*, 13.3, JFST0013.

Koshizuka, S. and Oka, Y. (1996). Moving-particle semi-implicit method for fragmentation of incompressible fluid. *Nuclear science and engineering*, 123(3), pp. 421–434.

Koshizuka, S. et al. (2018). Moving Particle Semi-implicit Method. *1st ed. Amsterdam: Elsevier*, pp.12-16.

Oochi, M. et al. (2010). Explicit MPS algorithm for free surface flow analysis. *Transactions of the Japan Society for Computational Engineering and Science*, 2010, 20100013, 8 pages (In Japanese).

Pasandideh-Fard et al. (2002). A three-dimensional model of droplet impact and solidification. *International Journal of Heat and Mass Transfer*, pp. 2229–2242.

Shakeri, S. and Chandra, S. (2002). Splashing of molten tin droplets on a rough steel surface. *International Journal of Heat and Mass Transfer*, 45.23, pp. 4561–4575.

Sundaram et al. (2007). Effects of surface deposition, hole blockage, and thermal barrier coating spallation on vane endwall film cooling. *Journal of Turbomachinery*, 129.3, pp. 599–607.

Tanaka, M. et al. (2009). Multi-resolution MPS Method. *Transactions of JSCES*, pp. 2–4.